Journal of Materials Chemistry

Dynamic Article Links

Cite this: *J. Mater. Chem.*, 2012, **22**, 10918

www.rsc.org/materials

PAPER

CO_2-selective free-standing membrane by self-assembly of a UV-crosslinkable diblock copolymer†

Baolong Xue,‡[a] Xianwu Li,‡[a] Longcheng Gao,*[a] Min Gao,[a] Yao Wang*[a] and Lei Jiang[ab]

Received 19th February 2012, Accepted 28th March 2012
DOI: 10.1039/c2jm31037f

A polyethylene oxide-*b*-polystyrene (PEO-*b*-PS) block copolymer incorporating UV-crosslinkable coumarin groups in the PS block self-assembled into a cylindrical structure with PEO cylinders perpendicular to the film surface, which exhibited excellent CO_2 separation properties. The block copolymer was successfully synthesized by atom transfer radical polymerization (ATRP). The molecular characterization of the diblock copolymer was performed with ^1H nuclear magnetic resonance (NMR) and gel permeation chromatography (GPC). The UV-crosslinking of the film was monitored by UV-vis absorption spectroscopy. The cylindrical phase structure was confirmed by transmission electron microscopy (TEM). Gas permeation properties of CO_2, N_2 and He were determined at different temperatures varying from 20 °C to 70 °C. Both the CO_2 permeation flux and total gas selectivity increased with increasing temperature. The maximum of CO_2 permeance at 70 °C was 20400 × 10^{-6} cm^3 cm^{-2} s^{-1} $cmHg^{-1}$, and gas selectivity over He and N_2 was 20.1 and 27.7, respectively. It was concluded that the functional block units and self-assembled microphase structures synergetically played key roles in the high performance of the membrane.

Introduction

CO_2 is known as the major greenhouse gas responsible for global warming. Many technologies for removing CO_2 from flues and natural gas streams are available, in which membrane separation is an outstanding technology for CO_2 capture. During the last two decades, many new polymers have been developed for gas separation membranes, which have been described in the literature.[1] Segmented block copolymers containing PEO have been widely investigated for the removal of CO_2 from other gases.[2–8] The ether oxygen linkages in PEO exhibit favorable interactions with CO_2 compared to gases like H_2, He, N_2 and CH_4.[1,9,10] Thus, the polymeric membranes have high CO_2 permeability and high selectivity over other gases. The gas-transport properties of these block copolymers can be tailored by controlling the crystallinity of the copolymers, the content and molecular weight of the EO segments and their microstructures.[2,4,11–13] In order to achieve high performance, the multiblock copolymers should contain a high content of EO units as an amorphous phase.[14–16] However, PEO with high molecular weight has a strong tendency to crystallize, which limits the amount of permeable amorphous soft phase and moreover reduces the chain mobility, resulting in strongly reduced gas permeability and selectivity. There have been ways to depress crystallization, such as blending liquid PEO with compatible solid polymers,[17] incorporating PPO randomly,[18] crosslinking PEO to form a network,[9] and so on. On the other hand, most of these segmented block copolymers have been synthesized by polycondensation reaction, resulting in a wide range of molecular sizes. The microphase separation structures cannot be as well controlled as those in diblock copolymers systems. There are defects and interfaces between the PEO domains.

Diblock copolymers, bearing chemically different polymers covalently bonded at a single point, can be synthesized by living polymerization, such as anionic/cationic polymerization, atom transfer radical polymerization (ATRP), *etc.* By precisely controlling the molecular weight and weight fraction of one block, a relatively narrow polydispersity can be realized. They can self-assemble into ordered nanostructures, related to the volume fraction of components, as well as the interaction parameter.[19,20] The domain sizes can be tuned easily by changing the molecular weights of the copolymers. By using external fields, such as solvent evaporation,[21] graphoepitaxy,[22] *et al.*, PS-PEO self-assembles into a hexagonally-packed cylindrical phase with PEO cylindrical microdomains oriented perpendicularly to the surface of the film. Considering that PEO has favorable interactions with CO_2, the well ordered microphase separation structures can be used as CO_2 transporting channels, when the film is free-standing.

[a]*Key Laboratory of Bio-inspired Smart Interfacial Science and Technology of Ministry of Education, School of Chemistry and Environment, Beihang University, Beijing, 100191, P. R. China. E-mail: lcgao@buaa.edu.cn; yao@buaa.edu.cn.*
[b]*Beijing National Laboratory for Molecular Sciences (BNLMS), Key Laboratory of Organic Solids, Institute of Chemistry, Chinese Academy of Sciences, Beijing, 100190, P. R. China*

† Electronic supplementary information (ESI) available. See DOI: 10.1039/c2jm31037f

‡ These authors contributed equally to this work.

Up to now, well-defined nanostructures self-assembled from block copolymers for CO_2 separation have been rarely reported. In this article we investigated the CO_2 transporting properties in phase-segregated diblock copolymer membranes with perpendicularly oriented PEO cylindrical domains. We chose moderate molecular weight PEO ($M_n = 2000$) as one block, and PS as the matrix. In order to get free-standing films, and also for physical and mechanical considerations, UV-crosslinkable coumarin units were statistically placed along the PS chains (see Scheme 1). Once the self-assembled structure was formed, UV-crosslinking the matrix surrounding the cylindrical microdomains maintained the original periodicity and enhanced the thermal and solvent durability. In this way, free-standing membranes can be obtained, thereby offering great facilities for successive application.[23–25]

Experimental

Materials

Chlorobenzene (Analytical purity, Beijing Chemical Reagents Co.) was treated with powdered CaH_2 and distilled before use. Toluene, THF (Analytical purity, Beijing Chemical Reagents Co.) were distilled from Na/benzophenone under N_2. CuBr was synthesized from $CuBr_2$. Cellulose acetate (CA, Analytical purity, Beijing Chemical Reagents Co.), 7-hydroxyl-4-methylcoumarin (Analytical purity, Beijing Chemical Reagents Co.), *N*,*N*′,*N*′,*N*″,*N*″-pentamethyldiethylenetriamine (PMDETA, 99.5%, TCI), 1-(chloromethyl)-4-vinylbenzene (97%, Aldrich), were used as received. Styrene (Analytical purity, Beijing Chemical Reagents Co.) was distilled prior to use. Membrane support Anodisc™ membrane filter with nanopores (0.020 μm in diameter) was purchased from Whatman International Ltd., Germany and used directly.

Measurements

All of the characterization methods, such as ^{1}H NMR spectroscopy, GPC, differential scanning calorimetry (DSC), TEM, absorption spectroscopy, used in this study were similar to those reported previously.[26]

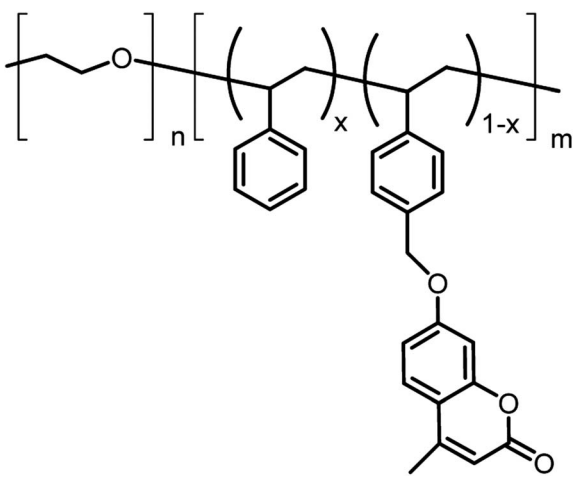

Scheme 1 The chemical structure of a UV-crosslinkable block copolymer containing coumarin units.

Synthetic procedures

Synthesis of UV-crosslinkable monomer coumarin-derived styrene (St-C) was achieved by coupling of coumarin and 1-(chloromethyl)-4-vinylbenzene.[27] Synthesis of macroinitiator PEO-Br was done following the literature.[28]

Synthesis of block copolymer. 1.65 g PEO-Br macroinitiator ($M_{n,\,GPC} = 2.1$k, PDI = 1.09, 0.78 mmol) was dissolved in 7.40 g of chlorobenzene. Then 6.67 g styrene (66.7 mmol), 1.00 g of St-C (6.5 mmol), 0.11 mg of CuBr (0.76 mmol) and 0.13 g of PMDETA (0.75 mmol) were added. The mixture was degassed by three freeze–pump–thaw cycles, and sealed under vacuum. The reaction tube was placed in an oil bath at 90 °C for 3 h. The polymerization was quenched by dipping the tube in ice/water and the tube was broken. The mixture was diluted with THF, passed through a basic alumina column, and precipitated into methanol. The block copolymers were filtered and dried under vacuum. The resulting product had MW of 8.7k, and PDI of 1.19 determined by GPC, and PEO blocks weight fraction was 29.6% determined by ^{1}H NMR.

Thin film sample preparation. On a silicon wafer, CA film was spin-coated from 4 wt% acetone solution at 1000 rpm. CA can dissolve in acetone but not in toluene. Then the copolymer film was made by spin-coating 4% toluene solutions onto the CA film at 1000 rpm. In order to get cylindrical PEO domains oriented normal to the surface, the film was placed in benzene vapor for 2 h at room temperature, dried in N_2 atmosphere overnight, and then under vacuum while the temperature was elevated gradually from ambient to 80 °C. The crosslinking of the block copolymer film was carried out by exposure to UV light ($\lambda = 365$ nm) for the desired time. After that, CA was dissolved using acetone without any damage to the block copolymer film. Then a free-standing film was obtained.

The UV-crosslinking of the film was monitored by UV-vis absorption spectroscopy (300 to 450 nm). The block copolymer film was spin coated onto a glass slide, and treated the same as described above.

Permeation measurements

Gases permeation measurements were based on the author's previous works and carried out with a home-built stainless steel permeation apparatus (Fig. S3†).[29–31] The pure gases studied were He, N_2 and CO_2. A membrane to be measured was placed in the permeation cell between two rubber O-rings with a support screen. The free standing film was put on a nanoporous Anodisc™ membrane filter in order not to be damaged by the gas flow. The surface area of the sample available for gas transporting was 2.8 cm^2. The membrane was placed in the cell at the high pressure side of the pressure gradient. The pressure gradient that was applied to each membrane was 3.0 psi. After passing through the membrane, the gaseous permeant was directed into a glass U-tube flow meter ($A_{col} = 1.0$ cm^2). The volumetric flow rate of the gas was then measured by recording the time

($t = t_f - t_i$) that was required for a soap bubble to travel a set distance ($X_{col} = d_f - d_i$), thereby sweeping out a defined volume. Measurements were taken until steady-state values were achieved (typically 1 to 2 h). At least six volumetric flow rates were recorded for each membrane, and the mean and standard deviations were determined. The error in each case was <5%. The permeation rate, P (10^6 cm^3 cm^{-2} s^{-1} cmHg^{-1}), was calculated using:

$$P = \frac{X_{col}A_{col}}{t\frac{76p}{14.7}A_{mem}} \times 10^6$$

This procedure was repeated for the next permeant gas. In general, the permeation properties were first measured for He, then for N_2, and finally for CO_2. The ideal selectivity (α) of CO_2 over another gas, B, was defined as:

$$\alpha = \frac{P_{CO2}}{P_B}$$

Discussion

The synthesis of the block copolymer was carried out by ATRP with PEO macroinitiator. The UV-crosslinkable monomer is a kind of styrene-based monomer. Therefore, it can be incorporated into the copolymer by ATRP. The content was controlled by the feed ratio with styrene. The molecular weight and molecular weight distribution were determined by GPC (Fig. 1).

The successful incorporation of crosslinkable groups was determined by ^{1}H NMR (Fig. 2). The characteristic peak at δ = 2.4 ppm was assigned to the methylene protons in the coumarin group, around δ = 5.0 ppm corresponded to the benzyl protons, and δ = 6.2 ppm corresponded to the proton of double bond (C=CH) adjacent to carbonyl group.

The UV-crosslinking of the film was monitored by UV-vis absorption spectroscopy. The typical coumarin absorption band appears from 300 to 360 nm. Fig. 3 illustrates the UV-vis absorption spectra of the block copolymer film under >300 nm irradiation. A nonlinear decrease of the 320 nm absorption band was assigned to the π–π^* transition of the coumarin unit (Fig. S1†). This photoreaction can be explained by the dimerization of the coumarin moieties through the [2 + 2] cyclization of the double bond.[32] The dimerization of the coumarin moieties caused UV-crosslinking in the polymer film and the film became insoluble in organic solvent. In this way, a free-standing membrane was obtained (Fig. 4). Films with arbitrary size can be obtained depending on the substrates.

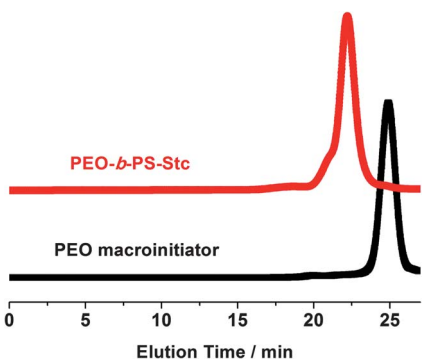

Fig. 1 Overlay of GPC traces for PEO macroinitiator and block copolymer.

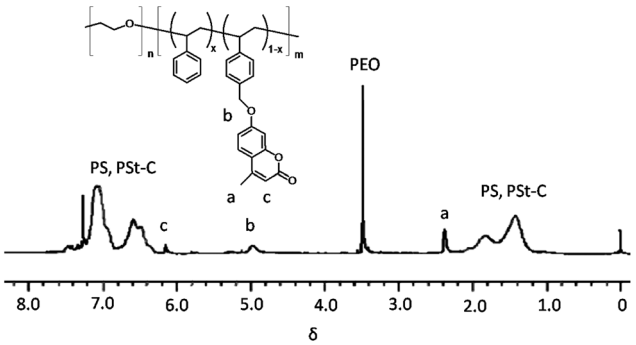

Fig. 2 ^{1}H NMR of block copolymer based on PEO ($CDCl_3$, 300 MHz).

Phase separation

The self-assembled structure of the block copolymer in the film was determined by TEM. Fig. 5 gives strong evidence of the microphase separation structures. The bright domains were PS and the dark ones were PEO because the PEO domains are stained dominantly with RuO_4 vapor to give a clear contrast. PEO chains can be stained by RuO_4 and PEO chains are more sensitive to RuO_4.[33] According to the weight fraction of the block copolymer (29.6 wt% of PEO), PEO formed cylinders in the PS matrix, with the cylindrical PEO domains oriented perpendicularly to the surface. Solvent evaporation has been proven to be a strong, highly directional method, which can produce arrays of cylindrical domains with perpendicular orientation.[21,34] Due to the nonselectivity and surface topographical fluctuation of the sacrificed CA substrate, liquid-like arrays of cylinders were obtained. Besides hexagonally packed cylinders, pentagonal and heptagonal arrangements of cylinders were also abundant. Although the cylinders lost the long range order, the basic requirement of perpendicular PEO cylinders throughout the film was realized.

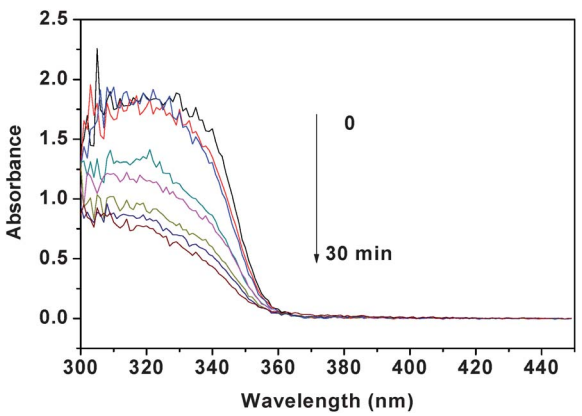

Fig. 3 Photoreaction of the block copolymer with irradiation at >300 nm. The irradiation times were 0, 0.5, 2.5, 3.5, 5.5, 7.5, 15, and 30 min.

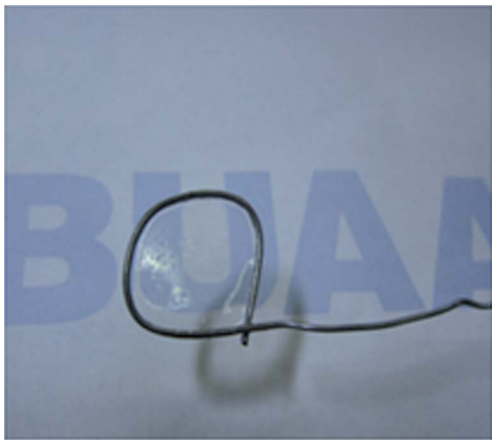

Fig. 4 Digital photograph of free-standing film detached from silicon wafer by dissolving the CA sacrificial layer.

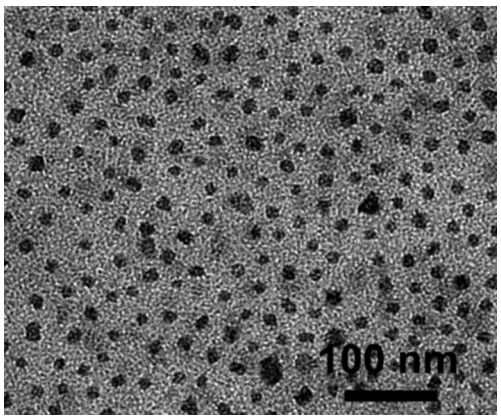

Fig. 5 TEM image of block copolymer film, indicating cylinders perpendicular to the surface (PEO was selectively stained by RuO_4).

Gas permeation

PEO has been regarded as a versatile building block to prepare highly permeable and sufficiently selective membranes for CO_2 permeation. For the first time, we fabricated a self-assembled membrane with perpendicularly oriented PEO cylinders as CO_2 transporting channels. The average thickness of the tested film was 1.6 μm by cross-section view from scanning electron microscopy (SEM).

Considering that PEO crystallinity strongly influenced gases permeation, elevated temperature measurement was carried out to reduce the PEO crystal/semi-crystal. The pure gases permeation and CO_2 selectivity of the film at various temperature are listed in Table 1. CO_2 permeability increased dramatically as the temperature increased (Fig. 6). At room temperature, the membrane had a permeance of 2160 $\times$ 10^{-6} cm^3 cm^{-2} s^{-1} $cmHg^{-1}$. When the temperature reached 70 °C, the permeance increased by ten times to 20400 $\times$ 10^{-6} cm^3 cm^{-2} s^{-1} $cmHg^{-1}$. No melting point of PEO was observed from DSC (Fig. S2†), so PEO was in a noncrystalline soft phase. When the temperature increased, the PEO became more flexible, resulting in higher CO_2 permeability. In contrast, the permeability of He and N_2 was much lower, because the polar EO units do not favor the solubility of these gases, so their solubility was significantly lower. Interestingly, both the permeances decreased as temperature increased (Fig. 6), different from the results previously reported.[7–9] This was related to the self-assembled structure, as we will show later.

Table 1 Permeances of gases across the polymer film at various temperatures

T/°C	CO_2[a]	He[a]	N_2[a]	CO_2/He[b]	CO_2/N_2[b]
20	2160	1700	1070	1.27	2.02
30	2610	1420	956	1.83	2.73
40	5140	1240	859	4.14	5.98
50	10700	1090	787	9.80	13.6
55	12700	1070	770	11.9	16.5
60	16400	1030	757	15.9	21.7
70	20400	1010	738	20.1	27.7

[a] Average permeances of gases, obtained from 6 independent measurements (10^6 cm^3 cm^{-2} s^{-1} $cmHg^{-1}$). [b] The pure gas selectivity.

The membrane exhibited high CO_2 selectivity over N_2 and He, which became even greater as the temperature increased (Fig. 7). The kinetic diameters of He, CO_2 and N_2 are 0.260, 0.330, and 0.363 nm, respectively.[35] Thus, based on Knudson diffusivity, the permeation rates should be He > CO_2 > N_2. He was chosen as a surrogate for H_2 (0.289 nm diameter) because He has similar size and permeation behavior as H_2; furthermore, He is non-combustible. The selectivity of $\alpha_{CO2/N2}$ at 20 °C was 2.02, and increased to 27.7 at 70 °C. Meanwhile, $\alpha_{CO2/He}$ was 1.27 at 20 °C, and increased to 20.1 at 70 °C.

The gas selectivity is mainly based on two main factors. The first one is the solubility selectivity, which is related to the favorable interactions of the EO units with CO_2; and the second one is diffusivity selectivity, which is influenced by the free volume. For the solubility selectivity, when the temperature increased, the interactions between EO units and CO_2 increased. In contrast, those of N_2 and He decreased. The solubility selectivity increased with rising temperature. For the diffusivity selectivity, as we know, the free volume increases in PEO domains and hard domains when temperature increases in the thermal-plastic segmented block copolymers system. Thus, the

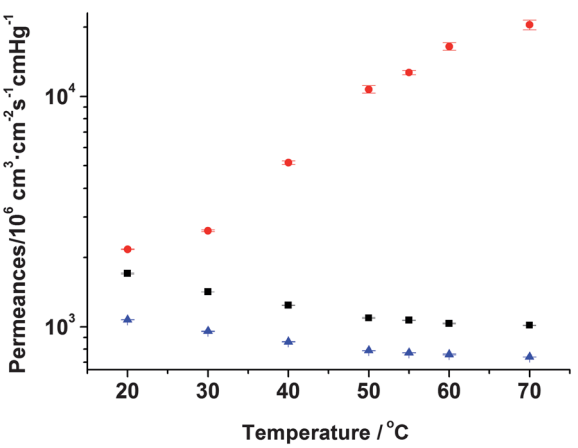

Fig. 6 Gas permeances for CO_2 (●), N_2(■), He (▲) as a function of temperature, indicating that CO_2 had the opposite tendency compared to that of N_2 and He.

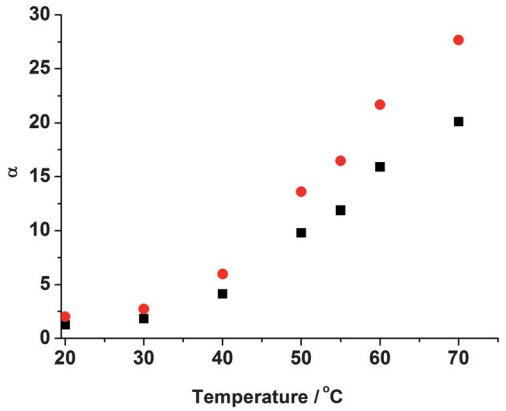

Fig. 7 Gas selectivity of $\alpha_{CO2/N2}$ (●) and $\alpha_{CO2/He}$ (■) as a function of temperature, indicating that CO_2 selectivity increases as temperature increases.

diffusivity for all the gases will increase. CO_2/light gases diffusivity selectivity would decrease as a result of the larger kinetic diameter of CO_2 than the light gases, especially He, as described in literature.[7–9] However, in our system, the PEO was confined in the cylinders surrounded by the crosslinked PS wall. Fig. 8 shows the schematic representation of the self-assembled structure and gases transport. When temperature increased, crosslinked PS continuous domains remained almost unchanged. PEO became more flexible, and chain segmental mobility increased in the confined cylindrical space. Furthermore, CO_2 could plasticize PEO, causing it to become more flexible. Therefore, CO_2 transport increased markedly. However for He and N_2, faster mobility of EO segments means denser barriers, and the chances that gases molecules get into the free volume decrease, leading to the reduced permeability. In summary, when temperature increased, the PEO cylinders became more philic for CO_2, and more phobic for He and N_2. CO_2 can be easily dissolved and diffuse in the PEO cylinders, while N_2 and He cannot easily do so. In this way, a new kind of CO_2 transporting nanochannel throughout the membrane, which was self-assembled by the block copolymer, was achieved. Due to the nanochannels, the membrane exhibited

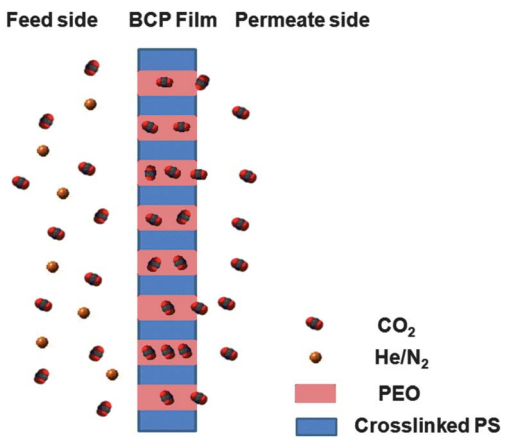

Fig. 8 Schematic representation of self-assembled film with PEO cylinders perpendicular to the film surface and CO_2 separation from light gases (He/N_2).

comparable CO_2 separation performances even though the PEO content was much lower than that of segmented block copolymers. What's more, the membrane thickness can be thin, because of the crosslinking of the PS matrix. The membrane had better performances at high temperature. This offers an opportunity of application in purifying hot post-combustion flue gas.

Conclusions

In conclusion, a kind of UV-crosslinkable diblock copolymer was successfully synthesized by ATRP, with the coumarin groups randomly located along the PS chain. The block copolymers self-assembled into a cylindrical structure with PEO cylinders oriented perpendicular to the surface. Taking advantage of the PEO cylinders, the film exhibited higher CO_2 diffusivity than N_2 and He. Due to the unique structure, both the CO_2 diffusivity and total gas selectivity increased with increasing temperature. Further exploitation of this feature is currently under investigation.

Acknowledgements

This work was supported by Specialized Research Fund for the Doctoral Program of Higher Education (20111102120050 and 20101102120043), the National Natural Science Foundation of China (51073006), Program for New Century Excellent Talents in University (2010), the Fundamental Research Funds for the Central Universities and Beijing Natural Science Foundation (2123063).

References

1 H. Lin and B. D. Freeman, *J. Mol. Struct.*, 2005, **739**, 57.
2 S. J. Metz, M. H. V. Mulder and M. Wessling, *Macromolecules*, 2004, **37**, 4590.
3 A. Car, C. Stropnik, W. Yave and K. V. Peinemann, *J. Membr. Sci.*, 2008, **307**, 88.
4 A. Car, C. Stropnik, W. Yave and K. V. Peinemann, *Adv. Funct. Mater.*, 2008, **18**, 2815.
5 D. Husken, T. Visser, M. Wessling and R. J. Gaymans, *J. Membr. Sci.*, 2010, **346**, 194.
6 V. I. Bondar, B. D. Freeman and I. Pinnau, *J. Polym. Sci., Part B: Polym. Phys.*, 2000, **38**, 2051.
7 S. R. Reijerkerk, A. Arun, R. J. Gaymans, K. Nijmeijer and M. Wessling, *J. Mater. Sci.*, 2010, **359**, 54.
8 H. Y. Zhao, Y. M. Cao, X. L. Ding, M. Q. Zhou and Q. Yuan, *J. Mater. Sci.*, 2008, **323**, 176.
9 H. Lin, E. Wagner, B. D. Freeman, L. G. Toy and R. P. Gupta, *Science*, 2006, **311**, 639.
10 H. Lin and B. D. Freeman, *J. Membr. Sci.*, 2004, **239**, 105.
11 A. A. Deschamps, D. W. Grijpma and J. Feijen, *Polymer*, 2001, **42**, 9335.
12 M. E. Arnold, K. Nagai, B. D. Freeman, R. J. Spontak, D. E. Betts, J. M. DeSimone and I. Pinau, *Macromolecules*, 2001, **34**, 5611.
13 N. P. Patel, A. C. Miller and J. Spontak, *Adv. Funct. Mater.*, 2004, **14**, 699.
14 W. Yave, A. Car, S. S. Funari, S. P. Nunes and K.-V. Peinemann, *Macromolecules*, 2010, **43**, 326.
15 K. Okamoto, M. Fujii, S. Okamyo, H. Suzuki, K. Tanaka and H. Kita, *Macromolecules*, 1995, **28**, 6950.
16 C. Damain, E. Espuche, M. Escoubes, S. Cuney and J. P. Pascault, *J. Appl. Polym. Sci.*, 1997, **65**, 2579.
17 T. C. Merkel, V. I. Bondar, K. Nagai, B. D. Freeman and I. Pinnau, *J. Polym. Sci., Part B: Polym. Phys.*, 2000, **38**, 415.
18 A. C. IJzer, A. Arun, S. R. Reijerkerk, K. Nijmeijer, M. Wessling and R. J. Gaymans, *J. Appl. Polym. Sci.*, 2010, **117**, 1394.
19 F. S. Bates, *Science*, 1991, **251**, 898.

20 G. H. Fredrickson and F. S. Bates, *Annu. Rev. Mater. Sci.*, 1996, **26**, 501.
21 S. H. Kim, M. J. Misner, T. Xu, M. Kimura and T. P. Russell, *Adv. Mater.*, 2004, **16**, 226.
22 S. Park, D. H. Lee, J. Xu, B. Kim, S. W. Hong, U. Jeong, T. Xu and T. P. Russell, *Science*, 2009, **323**, 1030.
23 E. Harth, B. V. Horn, V. Y. Lee, D. S. Germack, C. P. Gonzales, R. D. Miller and C. J. Hawker, *J. Am. Chem. Soc.*, 2002, **124**, 8653.
24 U. Jeong, D. Y. Ryu, J. K. Kim, D. H. Kim, T. P. Russell and C. J. Hawker, *Adv. Mater.*, 2003, **15**, 1247.
25 J. M. Leiston-Belanger, T. P. Russell, E. Drockenmuller and C. J. Hawker, *Macromolecules*, 2005, **38**, 7676.
26 L. C. Gao, C. L. Zhang, X. Liu, X. H. Fan, Y. X. Wu, X. F. Chen, Z. H. Shen and Q. F. Zhou, *Soft Matter*, 2008, **4**, 1230.
27 Q. Fu, L. L. Cheng, Y. Zhang and W. F. Shi, *Polymer*, 2008, **49**, 4981.
28 S. Park, D. H. Lee, J. Xu, B. Kim, S. W. Hong, U. Jeong, T. Xu and T. P. Russell, *Science*, 2009, **323**, 1030.
29 Y. Wang, V. Janout and S. L. Regen, *Chem. Mater.*, 2010, **22**, 1285.
30 Y. Wang, E. Stedronsky and S. L. Regen, *J. Am. Chem. Soc.*, 2008, **130**, 16510.
31 Y. Wang, E. Stedronsky and S. L. Regen, *Langmuir*, 2008, **24**, 6279.
32 Y. Q. Tian, X. X. Kong, Y. Nagase and T. Iyoda, *J. Polym. Sci., Part A: Polym. Chem.*, 2003, **41**, 2197.
33 K. Iwasaki, A. Hirao and S. Nakahama, *Macromolecules*, 1993, **26**, 2126.
34 J. Peng, Y. C. Han, W. Knoll and D. H. Kim, *Macromol. Rapid Commun.*, 2007, **28**, 1422.
35 Y. Cui, H. Kita and K. Okamoto, *Chem. Commun.*, 2003, 2154.